Theor Ecol
DOI 10.1007/s12080-009-0038-4

ORIGINAL PAPER

Leading indicators of phytoplankton transitions caused by resource competition

Stephen R. Carpenter · William A. Brock · Jonathan J. Cole · Michael L. Pace

Received: 30 September 2008 / Accepted: 15 January 2009

Abstract Many important transitions in phytoplankton composition of lakes and oceans are related to shifts in nutrient supply ratios. Some phytoplankton transitions, such as cyanobacteria blooms in freshwater supplies and red tides in coastal oceans, are important for aquatic resource management. Therefore, it would be useful to have leading indicators which precede phytoplankton shifts and could be readily monitored in the field. We investigated potential indicators using a well-understood model of phytoplankton dynamics parameterized to mimic the transition toward cyanobacteria blooms in freshwater lakes. In stationary distributions, performance of the indicators depends on whether the species are capable of stable coexistence over a certain range of nutrient inputs. In transient simulations, however, indicators show consistent responses regardless of the possibility of stable coexistence. Leading indicators occurring 10 to 40 days prior to species shift include shift of lag-1 autoregression coefficient toward 0, low standard deviation, fluctuating skewness, and high kurtosis. These responses are different from those reported for critical transitions such as fold bifurcations. Thus, the indicators reveal clues to the mechanisms of important ecosystem transitions. In practice, indicators should be measured for multiple ecosystem variables, and interpretation of the indicators should be guided by experiments and mechanistic site-specific models to help resolve potential ambiguities.

Keywords Algae bloom · Automated sensors · Competition · Ecological sensors · Ecosystem monitoring · Indicators · Phytoplankton · Nutrients · Regime shift

S. R. Carpenter (✉)
Center for Limnology, University of Wisconsin,
Madison, WI 53706, USA
e-mail: srcarpen@wisc.edu

W. A. Brock
Department of Economics, University of Wisconsin,
Madison, WI 53706, USA

J. J. Cole
Cary Institute of Ecosystem Studies,
Box AB, Route 44A,
Millbrook, NY 12545, USA

M. L. Pace
Environmental Sciences, University of Virginia,
Charlottesville, VA 22901, USA

Introduction

Hutchinson (1961) was among the first to envision how intense competitive interactions among phytoplankton could be blunted by non-equilibrium conditions. Hence, shifts in environmental conditions along with competition, predation, and other ecological factors explain seasonal successions of phytoplankton communities (Sommer 1990; Kalff 2002). For example, in temperate lakes, a spring bloom is often generated by increased light, stabilized water column, and inputs of nutrients. The spring bloom eventually fades with a transition to a clear-water phase of grazer control with the phytoplankton shifting to small algae capable of withstanding high mortality through rapid growth. The clear-water community is later displaced by species with protective structures (e.g., colonies, chains, spines) that are resistant to grazing and adapted to the warmer, low-nutrient conditions that prevail in summer. The summer community is in turn replaced when autumn mixing provides new nutrient inputs that support another set of species. Similarly, patterns of bloom formation and phytoplankton succession are well known in the ocean,

Published online: 03 February 2009

reflecting seasonal variation in light, temperature, mixing, and grazers (Valiela 1995).

In contrast with predictable patterns of seasonal succession, the high intrinsic growth rates of phytoplankton provide the potential for rapid transitions. Eruptive blooms of phytoplankton are well known. These blooms lead to massive accumulations of algal biomass, degradation of water quality, and, in some cases, toxic effects on other organisms including humans (Sellner et al. 2003). In freshwater, toxic blooms of cyanobacteria are most notable (Paerl 1988; Hudnell 2008). In marine systems, numerous species of dinoflagellates as well as other taxa form so-called red tides and are prominent examples of harmful algal blooms (Hallaegraf 1993; Anderson et al. 2002; Sellner et al. 2003; Graneli and Turner 2006). These types of blooms in both inland and marine waters are far less predictable and extremely important for management of aquatic resources. While the drivers of nuisance blooms are often understood, their timing and magnitude can be highly variable and prediction remains elusive (Schofield et al. 1999).

Various models have been used for the dramatic shifts in species dominance seen in phytoplankton communities, and all of these models have some consistencies with field observations. One of the earliest examples is the paradox of enrichment whereby gradual nutrient additions lead to a bifurcation from a stable point to a stable cycle (Rosenzweig 1971). A model for cyanobacterial blooms based on nutrient and light competition produces a different kind of critical transition leading to alternative states through a fold bifurcation (Scheffer et al. 1997). Models of three trophic levels can easily lead to very complex attractors (Hastings and Powell 1991). Other models and data for phytoplankton suggest chaotic dynamics (Beninca et al. 2008; Huisman and Weissing 1999; Scheffer et al. 2003). All of these shifts are examples of critical transitions where gradual change in a parameter or a slow variable leads to a change from one kind of attractor to a different one (Scheffer 2008). Yet, perhaps, the simplest model of sharp transitions in phytoplankton communities is simple nutrient competition where one species gives way to another as the ratio of nutrient supply changes (Tilman 1978).

Studies of critical transitions in ecology have shown that certain statistical properties of observable time series change before the bifurcation as the key parameter moves gradually toward a critical value (Horsthemke and Lefever 1984; Berglund and Gentz 2005; Kleinen et al. 2003; Carpenter and Brock 2006; van Nes and Scheffer 2007). For example, in the one-dimensional case, the lag-1 autocorrelation and lag-1 autoregression coefficients move close to 1 (critical slowing down), variance spectra shift to lower frequencies (red shift), and variance, skewness and kurtosis increase. Therefore, these statistics are leading indicators of the impending change. In many ecological examples that have been studied, the real part of the largest eigenvalue of the system passes through zero at the time of the critical transition (Kleinen et al. 2003; Carpenter and Brock 2006; van Nes and Scheffer 2007; Carpenter et al. 2008). As this eigenvalue approaches 0, variance and skewness increase and the lag-1 autocorrelation and autoregression coefficients approach 1 (Carpenter and Brock 2006; Guttal and Jayaprakash 2008; van Nes and Scheffer 2007). In the usual model of resource-based competition among two groups of phytoplankton, it is not clear whether this will happen (Huisman and Weissing 2001). For example, in some cases, the dominant eigenvalue remains negative as the transition occurs (Huisman and Weissing 2001), suggesting that the behavior of the statistical indicators will be different from what has been seen in fold bifurcations. Yet species shifts due to resource competition are thought to be common in ecosystems and are arguably the simplest case of alternate stable states. Therefore, it is interesting to examine the behavior of indicators near a transition between two species competing for resources.

The purpose of this paper was to investigate the time series indicators of rapid phytoplankton transitions across nutrient gradients. We evaluate potential leading indicators using a well-understood model of phytoplankton dynamics parameterized to mimic the transition toward cyanobacteria blooms in freshwater lakes. We consider both stationary and transient conditions and present evidence for leading indicators that differ from those previously observed for fold bifurcations.

Model

The model is a particular case of resource competition models studied by Tilman (1982, 1988) and applied specifically to phytoplankton by Follows et al. (2007). The model studied here represents dynamics of two phytoplankton taxa and two nutrients, nitrogen and phosphorus, in a well-mixed volume of water. The dynamics follow

$$\begin{aligned}\frac{\mathrm{d}N}{\mathrm{d}t} &= S_{\mathrm{N}} - mN - \sum_j \mu_j \gamma_j A_j R_j - \sum_j \sigma_j \gamma_j A_j R_j \frac{\mathrm{d}W_j}{\mathrm{d}t} \\ \frac{\mathrm{d}P}{\mathrm{d}t} &= S_{\mathrm{P}} - mP - \sum_j \mu_j \gamma_j A_j - \sum_j \sigma_j \gamma_j A_j \frac{\mathrm{d}W_j}{\mathrm{d}t} \\ \frac{\mathrm{d}A_j}{\mathrm{d}t} &= -mA_j + \mu_j \gamma_j A_j + \sigma_j \gamma_j A_j \frac{\mathrm{d}W_j}{\mathrm{d}t}\end{aligned} \quad . \qquad (1)$$

State variables are inorganic nitrogen and phosphorus (N and P, respectively) and two phytoplankton species, A_j, where j can be 1 or 2. S is the input rate of nutrients, m is the outflow rate, μ_j is the growth parameter of species j, and γ_j is the nutrient effect on growth of species j. R_j is the ratio

of N to P in phytoplankton species j. Phytoplankton biomass is measured in phosphorus units.

The stochasticity is added to the realized growth rate of each species $\mu_{R,j}=\mu_j+\sigma_j$. W_j is a Wiener process for species j. The shocks are independent for the two phytoplankton species. When solving the equations numerically, each individual shock to phytoplankton appears with the opposite sign in the nutrient equations to ensure conservation of mass.

The nutrient effect is

$$\gamma_j = \min\left(\frac{N}{N+k_{N,j}}, \frac{P}{P+k_{P,j}}\right) \tag{2}$$

where $k_{N,j}$ and $k_{P,j}$ are half-saturation coefficients of N and P, respectively, for species j.

Tilman's 1982 and 1988 books make extensive use of a graphical technique for interpreting the two-species, two-nutrient case. Here, we summarize the computation of the key features of this graphical analysis. These computations apply to the deterministic version of the model. The stochastic terms are set to 0.

Step 1 is to compute the zero-net-growth isoclines, or ZNGIs. These are defined as the lines where a species' net growth is 0 when limited by one of the nutrients. In the case of our model, N and P are not substitutable, so the ZNGIs for each species define a rectangle in N,P space. To find these lines, set the algae rate equation from expression 1 equal to 0 for a single species limited by a single nutrient:

$$\frac{dA_j}{dt} = 0 = -m_j A_j + \frac{\mu_j A_j X}{k_X + X} \tag{3}$$

where X is the nutrient. Solve for X to find the ZNGI line:

$$X = \frac{m_j k_X}{\mu_j - m_j}. \tag{4}$$

By computing all four ZNGI lines (for N and P for each species), the two ZNGI boxes (one for each species) can be drawn (Fig. 1).

Step 2 is to imagine the lines where N and P are co-limiting for one species. These lines are often called "consumption vectors," but we will call them "co-limitation lines" because along these lines, both nutrients are equally limiting to a species. To find the co-limitation lines, set both nutrient rate equations from expression 1 equal to 0 for a single species. The result is:

$$P = \frac{S_P}{m_j} + \frac{N}{R_j} - \frac{S_N}{mR_j}. \tag{5}$$

Note that P is a linear function of N. This line gives the combination of N and P values that are co-limiting for a species at a given combination of input rates.

Step 3 is to set the coexistence lines for the two species to a point on the ZNGIs. The most interesting point for our purposes is the crossover point where the two ZNGIs intersect. Here, both species are at equilibrium, though the equilibrium may be stable or unstable. Call the coordinates of this crossover point N^* and P^*. To find the nutrient supply rates at this crossover point, substitute P^* and N^* for P and N in Eq. 5. Note there are two equations, one for each species. Solve this pair of equations for S_P and S_N. In our case, the algebra is simplified because we assume identical loss rates, m, for all nutrients and algae. The result is:

$$\begin{aligned} S_{N,\min} &= mN* \\ S_{P,\min} &= mP* \end{aligned}. \tag{6}$$

We use the subscript "min" for minimum because S_N and S_P must exceed these values for algae to grow.

Step 4 is to solve for the equilibrium values of both species at the point where the two ZNGIs cross. Set the

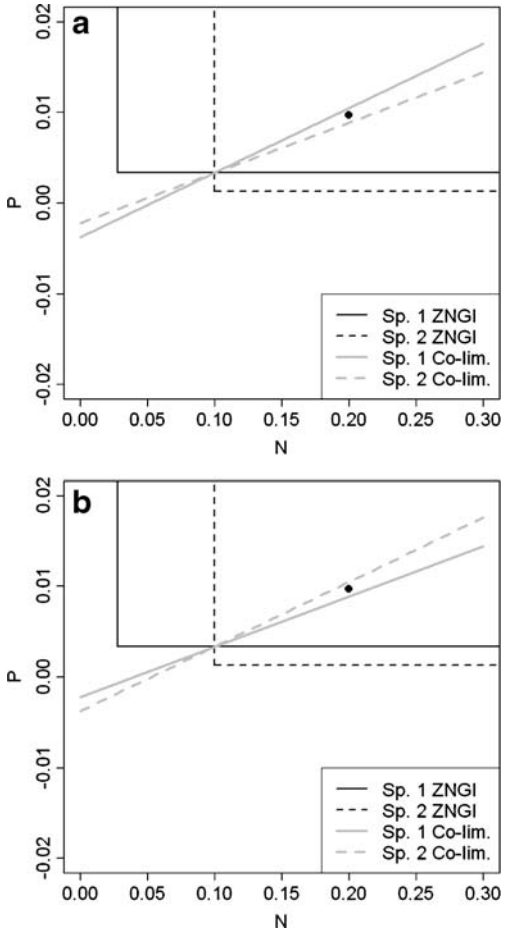

Fig. 1 Zero net growth isoclines (*ZNGIs*, *black*) and co-limitation lines (*gray*) for species 1 (*Sp. 1*, *solid*) and species 2 (*Sp. 2*, *dashed*) for a case of stable coexistence (**a**) and unstable transition between species (**b**). *Black dot* is an example of N*, P* values that lie between the co-limitation lines and above the ZNGIs

nutrient dynamics in Eq. 1 equal to zero, and solve simultaneously for the equilibrium values A_1* and A_2*. The result is:

$$A_1^* = \frac{(S_P - mP^* - \mu_2\gamma_2 A_2^*)}{\mu_1\gamma_1}$$
$$A_2^* = \frac{(S_N - R_1 S_P - mN^* + mR_1P^*)}{[\mu_2\gamma_2(R_1 - R_2)]}. \quad (7)$$

Note that if Eq. 6 is inserted in Eq. 7, the numerators are 0. For positive equilibrium values of algae, S_N and S_P must be chosen to be larger than the values defined by Eq. 6. If S_N and S_P are chosen so that $S_N > S_{N,min}$ and $S_P > S_{P,min}$, and the resulting N* and P* lie the wedge between the co-limitation lines and above all ZNGIs, the system can be stable or unstable (Fig. 1). Otherwise, the outcome is dominance by one species or disappearance of both species.

Step 5 is to evaluate the stability of the equilibrium. Stable coexistence requires that each species be more limited by a different nutrient (Tilman 1982, 1988). If one species has a higher uptake rate ($\mu_j\ \gamma_j\ A_j^*\ R_j$) for both nutrients, then that species is dominant and the equilibrium is unstable. Conversely, if each species has a higher uptake rate for the nutrient that most limits its growth, then the equilibrium is stable. This pattern is demonstrated by the analysis of Huisman and Weissing (2001, Appendix B). In their framework (with nitrogen as resource 2 and phosphorus as resource 1) and our notation, write the Jacobian in the case of Fig. 1a where species 1 is P-limited and species 2 is N-limited:

$$J = \begin{bmatrix} -A_1^* \frac{d\gamma_{P1}}{dP} & -A_1^* \frac{d\gamma_{P1}}{dP} \\ -R_1 A_2^* \frac{d\gamma_{N2}}{dN} & -R_2 A_2^* \frac{d\gamma_{N2}}{dN} \end{bmatrix}. \quad (8)$$

The eigenvalues of J are the solutions of

$$0 = \lambda^2 - Tr(J)\lambda + \det(J). \quad (9)$$

Both eigenvalues have negative real parts if $-\mathrm{Tr}(J) > 0$ and $\det(J) > 0$. The trace is obviously negative so the first condition holds. The determinant of J is

$$\det(J) = A_1^* \frac{d\gamma_{P1}}{dP} A_2^* \frac{d\gamma_{N2}}{dN}(R_2 - R_1). \quad (10)$$

The determinant is positive and the system is stable if $R_2 > R_1$, consistent with the outcomes in Fig. 1.

Simulation methods

The general strategy of the simulations is to compute indicator statistics across a gradient of P input rates while the N input rate is held constant. We expect to see shifts in indicators in the range of P input rates corresponding to the switch. The gradient of P input rate represents the situation in lakes where gradual P enrichment drives a transition from eukaryotic phytoplankton to blooms of nitrogen-fixing cyanobacteria. In the model, parameters were chosen so that species 2 is dominant at low P input rates and species 1 is dominant at high P input rates. Parameter values for the simulations are presented in Table 1.

We compare two scenarios. In one scenario, the species coexist stably for P input rates that place the system between the co-limitation lines (Fig. 1a). In the other scenario, there is no stable coexistence and the dominant species changes sharply when P input rates move the system through the co-limitation lines (Fig. 1b).

For each scenario, we compare indicators for stationary distributions and transient simulations. Stationary distributions sample time series under fixed rates of nutrient input near stochastic equilibrium, so the outcome should be unaffected by starting values (Horsthemke and Lefever 1984). Thus, the stationary distributions reveal the behavior of the indicators without the complications of changing inputs or transient dynamics. To simulate the stationary distributions, P input was held constant at a given value. Simulations were initiated at the deterministic equilibrium point and run for 5,000 time steps. The first 4,000 time steps were discarded and the last 1,000 time steps were used to compute the indicators. Transient simulations attempt to represent a field situation in which gradual changes in nutrient supply cause a shift in phytoplankton dominance. Thus, transient

Table 1 Parameter values used in simulations

Symbol	Definition	Units	Value
S_N	N input rate	$m\ v^{-1}\ t^{-1}$	4
S_P	P input rate	$m\ v^{-1}\ t^{-1}$	Varied
m	Outflow rate	t^{-1}	0.2
R_1	N/P ratio of species 1	m/m	14 (stable case) 18 (unstable case)
R_2	N/P ratio of species 2	m/m	18 (stable case) 14 (unstable case)
μ_1	Growth rate of species 1	t^{-1}	2
μ_2	Growth rate of species 2	t^{-1}	1.8
σ_1	Standard deviation of shocks to species 1	t^{-1}	0.01
σ_2	Standard deviation of shocks to species 2	t^{-1}	0.01
$k_{P,1}$	P half-saturation for species 1	m	0.03
$k_{P,2}$	P half-saturation for species 2	m	0.01
$k_{N,1}$	N half-saturation for species 1	m	0.25
$k_{N,2}$	N half-saturation for species 2	m	0.8

Units: m mass, v volume, t time

simulations reveal the behavior of indicators in a simplified representation of a field application, and outcomes depend on starting conditions and the rate of change in nutrient supply. For transient simulations, P input rate was gradually increased from 0.2 to 0.3 over 300 days (50 time steps per day). The indicators were computed from the 50 time steps sampled in each day.

All computations were performed in R (http://www.r-project.org/). Trajectories of the stochastic differential equations were computed by the Euler method using Ito stochastic calculus. We set σ=0.01 (Table 1) so that shocks were not likely to be large enough to overshadow effects of nutrient gradients, yet variability would be sufficient to compute statistics. Experiments with smaller and larger values of σ yielded patterns similar to those presented here. For both stationary and transient simulations, we computed standard deviation, coefficients of skewness and kurtosis, and lag-1 autoregression coefficient of total phytoplankton biomass. We also computed the correlation coefficient of the two species. For stationary simulations only, we computed the variance spectrum from the autocorrelation function. For the stationary distributions, all statistics were computed for the raw time series. For the transient simulations, statistics were computed for detrended (first-difference) time series to remove effects of non-stationarity.

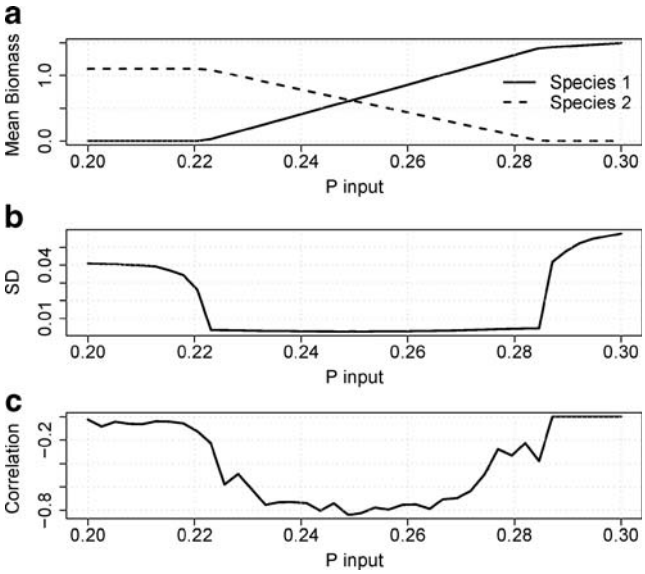

Fig. 2 Characteristics of the stationary distribution across a gradient of P input rate in a scenario where the species coexist stably at intermediate levels of P input rate. **a** Mean biomass of each species. **b** Standard deviation of total algae biomass (sum of both species). **c** Correlation coefficient of biomass of the two species

Simulation results

We first present the scenario where the species coexist stably at intermediate levels of P input. We start with the stationary distributions and then consider the transient simulations. Then, we turn to the second scenario where there is no stable coexistence, again starting with the stationary distributions and then the transient simulations.

Stable coexistence, stationary distributions

As the P input rate rises from about 0.22 to 0.28 (Fig. 2a), there is a gradual transition from dominance by species 2 (the superior competitor at high N/P ratio of inputs) to dominance by species 1 (the superior competitor at low N/P ratio of inputs). This range of P input rates corresponds to the zone between the co-limitation lines of Fig. 1a.

In the transitional range of P input rates, the standard deviation of total phytoplankton biomass (both species combined) decreases notably (Fig. 2b) and the correlation of the two species becomes more negative (Fig. 2c). The decrease in standard deviation may be explained, at least in part, by a statistical averaging effect (Doak et al. 1998). Specifically, the variance of the sum of random variables is equal to the sum of the variances plus twice the covariance which, in turn, is bounded above by the sum of the variances plus twice the product of the standard deviations. If the random variables are perfectly negatively correlated, then the variance of the sum is 0.

When one species of phytoplankton is dominant, the lag-1 autoregression coefficient of total phytoplankton biomass is slightly larger than −1 (Fig. 3a). When almost all the biomass is one species, a shock to growth of algae causes the opposite shock to nutrients, with an opposite effect on growth in the next time step. In the transitional range of P input rates, where the two species coexist, the lag-1 autoregression coefficient ranges from about −0.6 to +0.3 (Fig. 3a)

Skewness decreases as the system crosses the co-limitation lines (dips near 0.22 and 0.28; Fig. 3b). Kurtosis rises to high values while the system is between the co-limitation lines (Fig. 3c). In the same range of P input rates, variance spectra shift toward higher frequencies (Fig. 4).

Stable coexistence, transient simulations

In transient simulations, there is a gradual transition of species dominance between time steps (days) of about 75 and 160 (Fig. 5a). Starting about 10 to 15 time steps before the shift in dominance, there are several changes in time series statistics. The lag-1 autoregression coefficient moves from near −1 toward 0 (Fig. 5b), and the standard deviation is notably low (Fig. 5c). Skewness, which is near zero before and after the species transition becomes variable, either positive or negative (Fig. 6a). There is a notable increase in kurtosis (Fig. 6b).

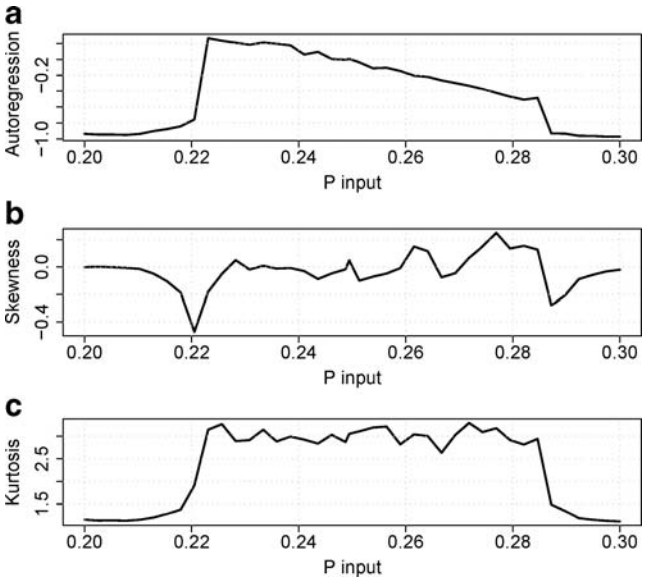

Fig. 3 Characteristics of the stationary distribution across a gradient of P input rate in a scenario where the species coexist stably at intermediate levels of P input rate. **a** Autoregression coefficient (lag 1) for biomass of total algae (both species combined). **b** Skewness of total algae. **c** Kurtosis of total algae

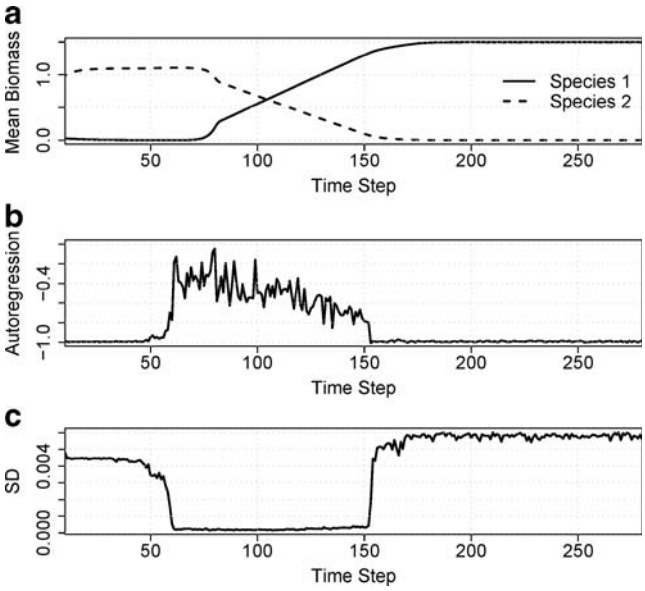

Fig. 5 Time series from a dynamic simulation in which P input rate is raised slowly from 0.2 to 0.3 for a scenario where the species coexist stably at intermediate levels of P input rate. **a** Mean biomass of each species. **b** Autoregression coefficient for total algae. **c** Standard deviation for total algae

Unstable transition, stationary distribution

In the unstable case, species dominance between the co-limitation lines depends on initial conditions as well as the magnitudes of P and N inputs. For the stationary simulations, there is a sharp shift in dominance near P input rate of 0.26 (Fig. 7a).

The behavior of the statistical indicators is strikingly different from the stable case. There is no discernible shift in the lag-1 autoregression coefficient near the transition (Fig. 7b). Standard deviation rises after the transition point (Fig. 7c), principally due to the higher growth rate of species 1. There is no discernible change in skewness at the transition point (Fig. 8a). Kurtosis has slightly different values on either side of the transition point (Fig. 8b). Spectra shift at the transition point (Fig. 9), with a greater proportion of variance at high frequencies when P input rates are larger than the transition point. This shift seems related to the higher growth rate of species 1.

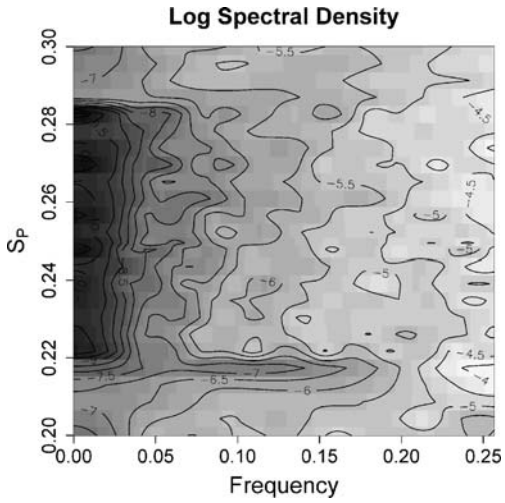

Fig. 4 Spectra of the stationary distribution of total algae across a gradient of P input rate, S_P, in a scenario where the species coexist stably at intermediate levels of P input rate. *X*-axis is frequency, *Y*-axis is P input rate S_P, and contours are spectral density. Spectral density is higher for *lighter shades*

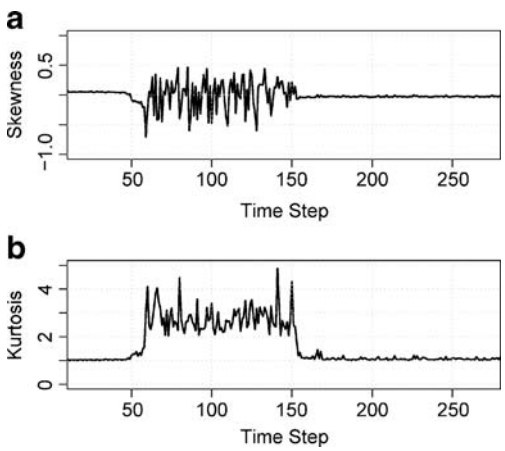

Fig. 6 Time series from a dynamic simulation in which P input rate is raised slowly from 0.2 to 0.3 for a scenario where the species coexist stably at intermediate levels of P input rate. **a** Skewness for total algae. **b** Kurtosis for total algae

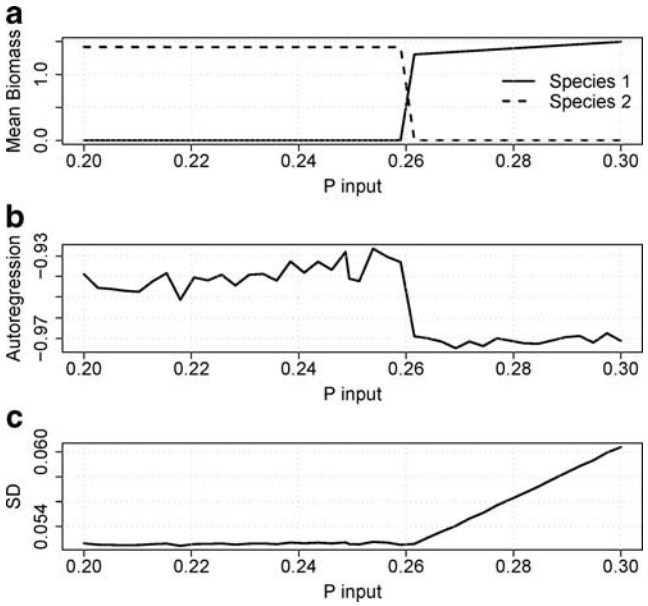

Fig. 7 Characteristics of the stationary distribution across a gradient of P input rate in a scenario where there is an unstable switch of dominance at an intermediate P input rate. **a** Mean biomass of each species. **b** Autoregression coefficient for total algae (lag 1). **c** Standard deviation of total algae

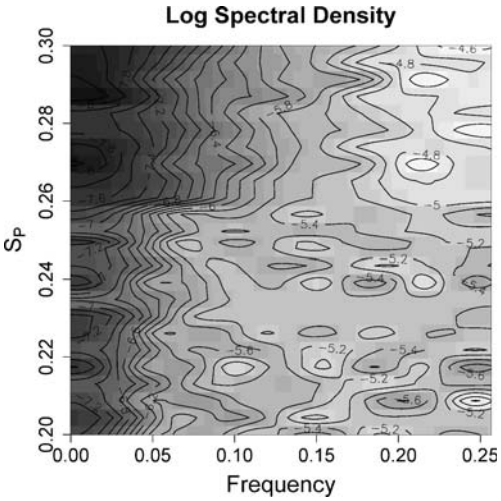

Fig. 9 Spectra of the stationary distribution of total algae across a gradient of P input rate, S_P, in a scenario where there is an unstable switch of dominance at an intermediate P input rate. *X*-axis is frequency, *Y*-axis is P input rate S_P, and contours are spectral density. Spectral density is higher for *lighter shades*

Unstable transition, transient simulation

In transient simulations of the unstable system, the shift of dominance occurs between time steps (days) about 180 and 220 (Fig. 10a). Even though the stationary distributions show minimal signals near the transition, there are notable changes in time series statistics well before the transition occurs. The lag-1 autoregression coefficient shifts from values near −1 toward 0, starting about day 140 (Fig. 10b).

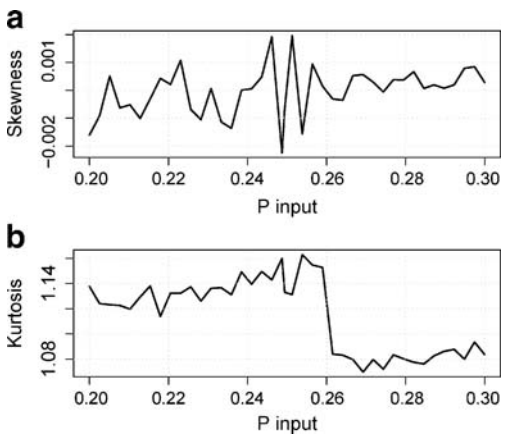

Fig. 8 Characteristics of the stationary distribution across a gradient of P input rate in a scenario where there is an unstable switch of dominance at an intermediate P input rate. **a** Skewness for total algae. **b** Kurtosis of total algae

The standard deviation decreases sharply about day 140 and remains low until about day 200 (Fig. 10c). Skewness is highly variable between about days 140 and 200 and otherwise is near zero (Fig. 11a). Kurtosis starts to increase about day 130 and is notably elevated between about days 150 and 200 (Fig. 11b).

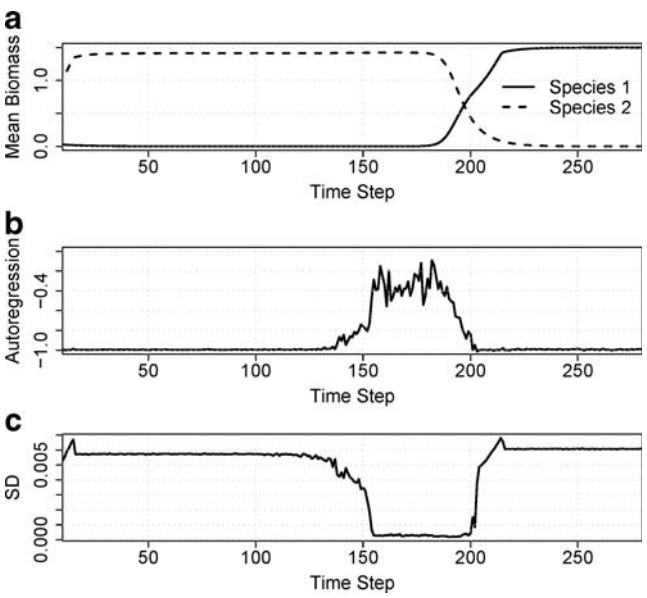

Fig. 10 Time series from a dynamic simulation in which P input rate is raised slowly from 0.2 to 0.3 for a scenario where there is an unstable switch of dominance at an intermediate P input rate. **a** Mean biomass of each species. **b** Autoregression coefficient for total algae. **c** Standard deviation for total algae

Discussion

Evaluation of model

In the stationary simulations, the performance of the indicators depends on whether the species can coexist stably. If stable coexistence can occur, then stationary distributions show different characteristics for the two-species case versus the one-species case. In the range of *P* inputs where the two species coexist, the standard deviation and skewness coefficient are relatively low, the kurtosis coefficient is relatively high, the lag-1 autoregression coefficient ranges from about −0.6 to +0.3, and variance spectra shift toward higher frequencies. The low standard deviation and interspecific correlation seem related to the limitation of the species by different nutrients. For example, a positive shock to the P-limited species also results in more uptake of *N* by that species, leading to an opposite shift in the N-limited species. The inverse correlations of the species in the zone of stable coexistence resembles the compensatory interactions among species that can stabilize production or other aggregate variables in some ecosystems (Ives et al. 2000). In contrast, when the species cannot coexist stably, then stationary distributions show little change at the transition point. There are small shifts in standard deviation, kurtosis, and spectra at the transition point, but these would be difficult to discern in field situations.

The changes in stationary distributions seen in transitions caused by resource competition are strikingly different from the behaviors seen in regime shifts caused by critical transitions such as fold bifurcations. Most previous studies of these indicators have examined regime shifts caused by fold bifurcations. Ecosystems undergoing fold bifurcations exhibit critical slowing down in which the dominant eigenvalue of the system passes through zero (van Nes and Scheffer 2007). In observed time series, fold bifurcations shift lag-1 autoregression coefficients very close to 1 (van Nes and Scheffer 2007; Carpenter et al. 2008). In phytoplankton competition, the lag-1 autoregression coefficient does not approach 1 during the transition.

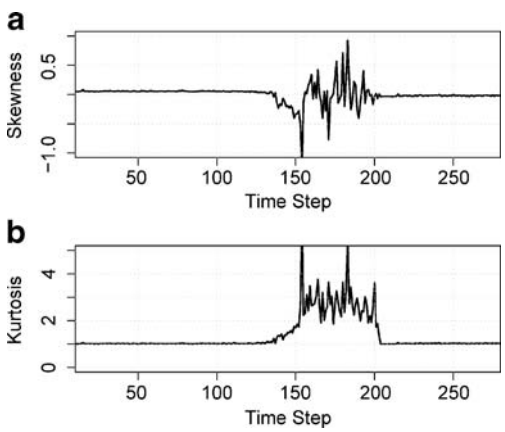

Fig. 11 Time series from a dynamic simulation in which P input rate is raised slowly from 0.2 to 0.3 for a scenario where there is an unstable switch of dominance at an intermediate P input rate. **a** Skewness for total algae. **b** Kurtosis for total algae

Other indicators perform differently as well. Fold bifurcations produce notable increases in variance (Carpenter and Brock 2006; Carpenter et al. 2008) and skewness (Guttal and Jayaprakash 2008) and shift spectra toward low frequencies (Kleinen et al. 2003; Carpenter et al. 2008). Resource competition produces opposite shifts when the species are capable of stable coexistence. For unstable competitive transitions, some indicators show no change and others can change in either direction, depending on the relative growth rates of the competing species. These differences suggest that the evolution of the eigenvalues during interspecific nutrient competition is different from that during fold transitions. Work on stability characteristics of multi-species resource competition systems suggests possibilities for great complexity, especially as more species and resources are considered (Beninca et al. 2008; Huisman and Weissing 1999, 2001; Scheffer et al. 2003). Further work is needed to understand changes in stability characteristics in relation to statistical indicators of impending transition in resource competition systems.

In transient simulations, for both the stable coexistence scenario and the unstable transition, the indicators signal the impending transition 10 to 40 days in advance. Prior to the transition, the lag-1 autoregression coefficient moves toward 0, standard deviation decreases, skewness becomes variable, and kurtosis increases. Thus, these statistics are leading indicators of dominance transition in phytoplankton communities. These warnings come early enough to be potentially useful in management. For example, warnings of a toxic algae bloom could be issued many days in advance of the bloom.

In transient simulations, the response of the indicators is similar to the stationary distributions for the stable coexistence case even if stable coexistence is not possible. Even in the case of unstable species replacement, the indicators' response is similar to the stable coexistence case. As the nutrient supply ratio changes very gradually near the transition point, shocks can cause switches between limitation by one nutrient or the other, and therefore dominance by one species or the other, for brief periods of time. Total phytoplankton has low standard deviation even though the species are switching dominance because the changes in the two species are inversely correlated. As a consequence, low standard deviations of total biomass occur before the transition point in transient simulations for both the stable and unstable cases. It is interesting that the indicators offer

the possibility of discriminating transitions due to resource competition from critical transitions associated with fold bifurcations. Resource competition transitions and critical transitions produce opposite shifts in standard deviations and spectra and different shifts in the lag-one autoregression coefficient.

Leading indicators in the field?

Our results suggest that some inferences about possible impending regime shift can be made from high-frequency time series of data on phytoplankton biomass alone. Consistent, sustained, in situ automated high-frequency measurement of key algal pigments has become routine in recent years. Automated, in situ, optical and fluorescent sensors that detect chlorophyll-a (a pigment common to all phytoplankton) are relatively inexpensive and reliable enough that they are deployed in many non-turbid environments in both lakes and the ocean (Johnsen and Sakshaug 2000; Chan and Un 2001). In some regions, networks of automated "smart-buoys" relay real-time pigment data to researchers on shore (Ciavatta et al. 2008; Porter et al. 2005). In addition to monitoring total algal pigments, both spectral filtering approaches and specific pigment sensors allow for real-time measurement of key algal groups (Aberle et al. 2006). Remote sensing approaches can provide data on pigments and, in some cases, specific algal groups at high frequency and large spatial scales (Lavender and Groom 1999; Hu et al. 2005; Kutser et al. 2006). At the cutting edge of this technology are sensors that provide genetic identification using real-time polymerase chain reaction (John et al. 2007; Oberholster and Botha 2007).

Although forecasting harmful algal blooms has been a goal for some time (Schofield et al. 1999), the technology for obtaining high-frequency observations has advanced farther and faster than the models needed to forecast blooms from leading indicators. Our approach is a first step. Data from the monitoring networks at times when known blooms occurred could be used to further test and refine the models. The leading indicator models may be expanded to capture information not only on total algal biomass but also variations in specific subgroups of phytoplankton within the community.

Next steps

We analyzed the specific case of *P* enrichment leading to a bloom of phytoplankton, such as cyanobacteria, that compete well under nitrogen limitation. However, patterns seen here should apply to resource-driven transitions between a pair of competing species that conforms to the assumptions of the model of resource competition which is widely used in the literature. In systems with three or more species and resources, dynamical outcomes can be more complicated (Beninca et al. 2008; Huisman and Weissing 1999, 2001; Scheffer et al. 2003). These more complex outcomes are likely to be more representative of field situations and therefore are worthy of ongoing study.

In complex field situations, responses of the indicators could be ambiguous. For example, a decline in standard deviation could signal a forthcoming competitive shift in dominance or movement of the ecosystem away from a threshold of critical transition. In order to interpret changes in the indicators for a given situation, it would be important to analyze and compare responses of time series for many ecosystem components at different levels of the food web and to couple time series analyses with experimental probes (when possible) and mechanistic models of ecosystem performance. Thus, inferences about ecosystem changes and early warnings may depend on site-specific information about the likely mechanisms of transitions.

Despite these complications, these indicators offer new tools for investigating mechanisms of transitions in ecosystems and perhaps providing early warnings of transitions that affect human use of ecosystems. These findings suggest that further investigation is warranted. We believe that theory must advance in close association with field studies to assess leading indicators of phytoplankton transitions. Situation-specific mechanistic models should be combined with field studies of important transitions (such as the well-known seasonal transitions or major blooms). On the basis of such studies, it should be possible to develop guidelines for measuring and interpreting indicators of incipient ecological transitions.

Acknowledgements We thank P.C. Hanson, A.R. Ives, C.T. Solomon and two anonymous referees for helpful comments, and the NSF for support.

References

Aberle N, Beutler M, Moldaenke C, Wiltshire KH (2006) 'Spectral fingerprinting' for specific algal groups on sediments in situ: a new sensor. Arch Hydrobiol 167:575–592. doi:10.1127/0003-9136/2006/0167-0575

Anderson DM, Glibert PM, Burkholder JM (2002) Harmful algal blooms and eutrophication: nutrient sources, composition, and consequences. Estuaries 25:704–726. doi:10.1007/BF02804901

Beninca E, Huisman J, Heerkloss R, Johnk KD, Branco P, van Nes EH, Scheffer M, Ellner SP (2008) Chaos in a long-term experiment with a plankton community. Nature 451:822–825. doi:10.1038/nature06512

Berglund N, Gentz B (2005) Noise-induced phenomena in slow-fast dynamical systems. A sample-paths approach. Springer, Berlin

Carpenter SR, Brock WA (2006) Rising variance: a leading indicator of ecological transition. Ecol Lett 9:311–318. doi:10.1111/j.1461-0248.2005.00877.x

Carpenter SR, Brock WA, Cole JJ, Kitchell JF, Pace ML (2008) Leading indicators of trophic cascades. Ecol Lett 11:128–138

Chan RKY, Un KM (2001) Real-time size distribution, concentration, and biomass measurement of marine phytoplankton with a novel dual-beam laser fluorescence Doppler cytometer. Appl Opt 40:2956–2965. doi:10.1364/AO.40.002956

Ciavatta S, Pastres R, Badetti C, Ferrari G, Beck MB (2008) Estimation of phytoplanktonic production and system respiration from data collected by a real-time monitoring network in the Lagoon of Venice. Ecol Modell 212:28–36. doi:10.1016/j.ecolmodel.2007.10.025

Doak DF, Bigger D, Harding EK, Marvier MA, O'Malley RE, Thomson D (1998) The statistical inevitability of stability–diversity relationships in community ecology. Am Nat 151:264–276. doi:10.1086/286117

Follows MJ, Dutkeiwicz S, Grant S, Chisholm SW (2007) Emergent biogeography of microbial communities in a model ocean. Science 315:1843–1846. doi:10.1126/science.1138544

Graneli E, Turner JT (eds) (2006) Ecology of harmful algae. Springer, New York, USA

Guttal V, Jayaprakash C (2008) Changing skewness: an early warning signal of regime shifts in ecological systems. Ecol Lett 11:450–460. doi:10.1111/j.1461-0248.2008.01160.x

Hallaegraf GM (1993) Review of harmful algal blooms and their apparent global increase. Phycologia 32:79–99

Hastings AM, Powell T (1991) Chaos in a three species food chain. Ecology 72:896–903. doi:10.2307/1940591

Horsthemke W, Lefever R (1984) Noise-induced transitions. Springer, Berlin

Hu CM, Muller-Karger FE, Taylor C, Carder KL, Kelble C, Johns E, Heil CA (2005) Red tide detection and tracing using MODIS fluorescence data: a regional example in SW Florida coastal waters. Remote Sens Environ 97:311–321. doi:10.1016/j.rse.2005.05.013

Hudnell HK (2008) Cyanobacterial harmful algal blooms: state of the science and research need. Advances in experimental medicine and biology, vol 619. Springer, New York, USA

Huisman J, Weissing FJ (1999) Biodiversity of plankton by species oscillations and chaos. Nature 402:407–410. doi:10.1038/46540

Huisman J, Weissing FJ (2001) Biological conditions for oscillations and chaos generated by multispecies competition. Ecology 82:2682–2695

Hutchinson GE (1961) The paradox of the plankton. Am Nat 95:137–146. doi:10.1086/282171

Ives AR, Gross K, Klug JL (2000) Stability and variability in competitive communities. Science 286:542–544. doi:10.1126/science.286.5439.542

John DE, Patterson SS, Paul JH (2007) Phytoplankton-group specific quantitative polymerase chain reaction assays for RuBisCO mRNA transcripts in seawater. Mar Biotechnol 9:747–759. doi:10.1007/s10126-007-9027-z

Johnsen G, Sakshaug E (2000) Monitoring of harmful algal blooms along the Norwegian coast using bio-optical methods. S Afr J Mar Science-Suid-Afrikaanse Tydskrif Vir Seewetenskap 22:309–321

Kalff J (2002) Limnology: inland water ecosystems. Prentice-Hall, Upper Saddle River, New Jersey, USA

Kleinen T, Held H, Petschel-Held G (2003) The potential role of spectral properties in detecting thresholds in the earth system: application to the thermohaline circulation. Ocean Dyn 53:53–63. doi:10.1007/s10236-002-0023-6

Kutser TL, Metsamaa N, Strombeck N, Vahtmae E (2006) Monitoring cyanobacterial blooms by satellite remote sensing. Estuar Coast Shelf Sci 67:303–312. doi:10.1016/j.ecss.2005.11.024

Lavender SJ, Groom SB (1999) The SeaWiFS automatic data processing system (SeaAPS). Int J Remote Sens 20:1051–1056. doi:10.1080/014311699212830

Oberholster PJ, Botha AM (2007) Use of PCR based technologies for risk assessment of a winter cyanobacterial bloom in Lake Midmar, South Africa. Afr J Biotechnol 6:1794–1805

Paerl HW (1988) Nuisance phytoplankton blooms in coastal, estuarine, and inland waters. Limnol Oceanogr 33:823–847

Porter J, Arzberger P, Hanson PC, Kratz TK, Gage S, Williams T, Shapiro S, Bryant P, Lin F, King H, Hanson T, Braun H, Michener W (2005) Wireless sensor networks for ecology. Bioscience 55:561–572. doi:10.1641/0006-3568(2005)055[0561:WSNFE]2.0.CO;2

Rosenzweig ML (1971) Paradox of enrichment: destabilization of exploitation ecosystems in ecological time. Science 171:385–387. doi:10.1126/science.171.3969.385

Scheffer M (2008) Critical transitions. Princeton University Press, Princeton, NJ, USA

Scheffer M, Rinaldi S, Gragnani A, Mur LR, van Nes EH (1997) On the dominance of filamentous cyanobacteria in shallow turbid lakes. Ecology 78:272–282

Scheffer M, Rinaldi S, Huisman J, Weissing FJ (2003) Why plankton communities have no equilibrium: solutions to the paradox. Hydrobiologia 491:9–18. doi:10.1023/A:1024404804748

Schofield O, Grzynski J, Bissett WP, Kirkpatrick GJ, Millie DF, Moline M, Roesler CS (1999) Optical monitoring and forecasting systems for harmful algal blooms: possibility or pipe dream? J Phycol 35:1477–1496. doi:10.1046/j.1529-8817.1999.3561477.x

Sellner KG, Doucett GJ, Kirkpatrick GJ (2003) Harmful algal blooms: causes, impacts, detection. J Ind Microbiol Biotechnol 30:383–406. doi:10.1007/s10295-003-0074-9

Sommer U (ed) (1990) Plankton ecology: succession in plankton communities. Springer, New York, USA

Tilman D (1978) Resource competition between phytoplanktonic algae: an experimental and theoretical approach. Ecology 58:338–348. doi:10.2307/1935608

Tilman D (1982) Resource competition and community structure. Princeton University Press, Princeton, New Jersey, USA

Tilman D (1988) Plant strategies and the dynamics and function of plant communities. Princeton University Press, Princeton, New Jersey, USA

Valiela I (1995) Marine ecological processes, 2nd edn. Springer, New York, USA

van Nes E, Scheffer M (2007) Slow recovery from perturbations as a generic indicator of a nearby catastrophic shift. Am Nat 169:738–747. doi:10.1086/516845